11th World Congress on Computational Mechanics (WCCM XI)
5th European Conference on Computational Mechanics (ECCM V)
6th European Conference on Computational Fluid Dynamics (ECFD VI)
E. Oñate, J. Oliver and A. Huerta (Eds)

STRUCTURAL ANALYSIS OF FROST DAMAGED CONSTRUCTIONS BY MEANS OF A COUPLED ENVIRONMENTAL-MECHANICAL DAMAGE MODEL

LUISA BERTO*, ANNA SAETTA*, DIEGO A. TALLEDO*
AND RENATO VITALIANI†

* Department of Architecture Construction Conservation (DACC) - University IUAV of Venice
Campus Terese, Dorsoduro 2206, 30123, Venice, Italy
e-mail: saetta@iuav.it

† Department of Civil, Environmental and Architectural Engineering - University of Padova
Via Marzolo 9, 35125 Padova, Italy

Key Words: *Freezing-and-thawing, reinforced concrete, coupled damage model.*

Abstract. During the last decades durability issues gained more interest and the necessity of reliable and suitable models for the prediction of concrete behaviour on time has grown. One of the most severe deterioration processes that may affect concrete structures is caused by freezing-and-thawing cycles. The causes and mechanisms of frost damaging process have been deeply studied during the last decades and different theories have been developed to describe the physical process of damaging due to frost action. Nevertheless very little attention has been given to the effect of frost attack on the behaviour of reinforced concrete (R/C) structures and on the material characteristics and bond properties of concrete. Recent studies showed that frost action leads to a reduction of compressive and tensile strength, an increasing of peak strain and fracture energy and a reduction of bond strength. In the present work an innovative formulation recently proposed by the authors within the framework of coupled environmental-mechanical damage approach is reorganized and further enhanced considering additional experimental tests in order to be more general. Furthermore the proposed model is used as a predictive tool to evaluate load carrying capacity of some frost damaged beams showing the robustness and efficacy of the numerical procedure in reproducing the main experimental evidenced of structural behaviour of R/C affected by action of freeze-and-thawing cycles (FTC).

1 INTRODUCTION

Reinforced concrete (RC) is one of the most common materials for constructions and was widely used, since the beginning of the last century, for both entire buildings and key structural elements that need to be able to resist considerable stresses. Even if initially it was considered an eternal material, during the last decades the problem of durability gained increasing attention. When RC constructions are exposed to aggressive environment, degradation processes may occur leading to several consequences that can even be extremely dangerous, also in regard to life safety requirements. Durability aspects are extremely important also in seismic prone areas; indeed it was observed that degradation processes may lead to a drastic reduction of both load-carrying capacity and ductility, compromising the seismic performance. Furthermore during the last decades more and more concrete structures are built in harsher environments. These considerations point out the necessity for reliable methods to study deteriorated RC structures. A lot of effort is being made both from the experimental and numerical point of view to contribute the advancement of knowledge and technology in this field.

Among the degradation processes that may affect RC constructions, experience shows that the most severe attacks on RC elements are those that lead to reinforcement corrosion (e.g. carbonation, chloride attack) and those causing internal cracking (often due to internal expansive actions), like sulphate attack and frost damage due to freezing-and-thawing cycles (FTC). The effect of FTC is gaining more interest in the last years also because there is an increasing need to build RC structures to contain very cold substances [1].

It is widely acknowledged that two different types of frost damage can be distinguished (e.g. [2]): internal damage and surface scaling. The first is generally caused by freezing of water contained in the pore system of concrete; on the other hand, the second is mainly caused by freezing of the concrete surface when it stays in contact with weak saline solution. It was observed that freezing in pure water often leads to internal damage but can seldom lead to surface scaling, while freezing in salt solution leads generally to surface scaling, but it can seldom lead to internal damage [2]. The effects of surface scaling are mainly the reduction of concrete cover and a reduction of anchorage capacity, but leaving undamaged the inner concrete. On the other hand, internal damage affects (e.g. [1-4]) compressive strength, tensile strength, elastic modulus, fracture energy, bond between reinforcement and concrete. Since only internal damage affects material properties, this work deals with this type of damage.

First the coupled environmental-mechanical damage model is briefly recalled. Second the enhanced formulation of the frost-damage model is presented. Third the model is calibrated considering some experimental results available in literature. Finally the proposed model is used as a predictive tool to simulate the structural behaviour of frost-damage beams. The experimental results are captured reasonably well, proving the reliability and efficacy of the proposed model.

2 ENVIRONMENTAL-MECHANICAL DAMAGE MODEL FOR CONCRETE

For readers' convenience, in this section the coupled environmental-mechanical damage model is briefly recalled. The constitutive model is developed within the framework of continuum damage mechanics: in particular it is a two-parameter isotropic plastic-damage model based on the strain equivalence concept. According to this, the effective stress tensor is defined as:

$$\bar{\boldsymbol{\sigma}} = \mathbf{C}_0 : \boldsymbol{\varepsilon}^e \tag{1}$$

where $\mathbf{C}_0$ is the fourth-order elastic stiffness tensor and $\boldsymbol{\varepsilon}^e$ is the elastic part of the total strain tensor, which is split according to:

$$\boldsymbol{\varepsilon} = \boldsymbol{\varepsilon}^e + \boldsymbol{\varepsilon}^p \tag{2}$$

The model takes into account both tensile and compressive failure mechanisms of concrete through the spectral decomposition of the effective stress tensor into a positive and a negative part:

$$\bar{\boldsymbol{\sigma}} = \bar{\boldsymbol{\sigma}}^+ + \bar{\boldsymbol{\sigma}}^- \tag{3}$$

According to the first law of thermodynamics, during a physical process the energy dissipation must be non-negative. Consequently, writing the Clausius-Duhem inequality, the following relation between Cauchy stress tensor and effective stress tensor can be written:

$$\boldsymbol{\sigma} = (1 - d^+)\bar{\boldsymbol{\sigma}}^+ + (1 - d^-)\bar{\boldsymbol{\sigma}}^- \tag{4}$$

where d^+ and d^- are the two scalar damage variables associated with tensile and compressive failure modes respectively.

The damage surface is defined by the following criterion:

$$g = \left(\frac{\tau^+}{r^+}\right)^2 + \left(\frac{\tau^-}{r^-}\right)^2 - 1 \leq 0 \tag{5}$$

where r^+ and r^- are the threshold variables that monitor the size of the expanding damage surface and τ^+ and τ^- are appropriate scalar measures of the effective stress tensor defined by:

$$\tau^+ = \sqrt{E\bar{\boldsymbol{\sigma}}^+ : \mathbf{C}_0^{-1} : \bar{\boldsymbol{\sigma}}^+} \tag{6}$$

$$\tau^- = \sqrt{\sqrt{3}(K\bar{\sigma}_{oct}^- + \bar{\tau}_{oct}^-)}$$

where E is Young modulus of concrete, $\bar{\sigma}_{oct}^-$ and $\bar{\tau}_{oct}^-$ are the octahedral normal stress and the octahedral shear stress of negative effective stress tensor respectively and K is a material parameter that accounts for the compressive strength increase due to biaxial compression and related to the ratio R_0 between 2D and 1D compressive strength.

The adopted evolution laws for the damage variables are:

$$d^+ = 1 - \left(\frac{r_0^+}{\tau^+}\right) \exp\left[A^+\left(1 - \frac{\tau^+}{r_0^+}\right)\right] \tag{7}$$

$$d^- = 1 - \left(\frac{r_0^-}{\tau^-}\right)^{0.5} (1 - A^-) - A^- \exp\left[B^-\left(1 - \left(\frac{\tau^-}{r_0^-}\right)^{0.5}\right)\right]$$

where r_0^+, A^+, r_0^-, A^- and B^- are parameters of the model. For their meaning readers can refer to [6-8].

Extending previous works (e.g.[7]), the coupling of environmental degradation with mechanical behaviour is obtained defining an additional scalar damage parameters, d_{env} which affect the positive and negative part of the effective stress tensor according to the following relation:

$$\boldsymbol{\sigma} = (1 - d_{env})(1 - d^+)\bar{\boldsymbol{\sigma}}^+ + (1 - d_{env})(1 - d^-)\bar{\boldsymbol{\sigma}}^- = (1 - d^{*+})\bar{\boldsymbol{\sigma}}^+ + (1 - d^{*-})\bar{\boldsymbol{\sigma}}^- \tag{8}$$

where d^{*+} and d^{*-} are the positive and negative coupled damage parameter respectively.

Independently from their specific definition, the environmental damage variables are represented by an increasing function with time, which means $\dot{d}_{env} \geq 0$. The effect of different levels of degradation, i.e. for different values of d_{env}, is depicted in Figure 1(a) and (b) respectively.

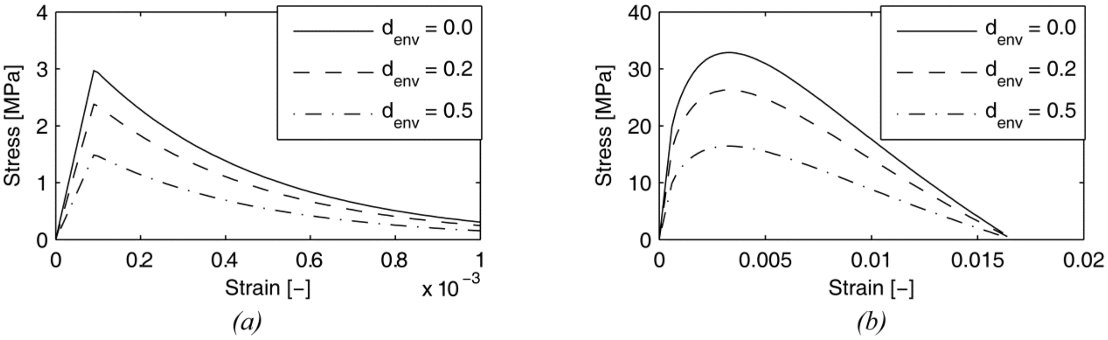

Figure 1: Stress-strain curves for different levels of degradation: *(a)* compression curve; *(b)* tension curve

Finally the model assumes that the damage criterion also describes the plastic surface so that the development of material damage is simultaneous with the accumulation of irreversible strains according to the following relation:

$$\dot{\boldsymbol{\varepsilon}}^p = \beta E H(\dot{d}) \frac{\langle \bar{\boldsymbol{\sigma}} : \dot{\boldsymbol{\varepsilon}} \rangle}{\bar{\boldsymbol{\sigma}} : \bar{\boldsymbol{\sigma}}} \mathbf{C}_0^{-1} : \bar{\boldsymbol{\sigma}} \tag{9}$$

where H is the Heaviside function, $\dot{d} = \dot{d}^+ + \dot{d}^-$ and $\beta \geq 0$ is a plastic strain coefficient that is assumed to be a model parameter. For more information about determination of β, readers can refer to [9].

3 FREEZE-AND-THAW DEGRADATION MODEL

Among the different effects of FTC on reinforced concrete introduced in section 1, in the present stage of the research, the proposed model is able to account for reduction of both elastic modulus and uniaxial and biaxial compressive strength, increasing of both peak deformation and ratio between biaxial and uniaxial compressive strength, and reduction of uniaxial tensile strength.

The parameters that control these aspects are d_{env}, β and R_0 which are here related to the frost degradation. In this stage of research the following relationships are proposed, e.g. [6]:

$$d_{env} = a_d \, N_{eq} \leq 1 \tag{10}$$

$$\frac{\beta}{\beta_{sound}} = a_\beta N_{eq} + 1 \leq \frac{1}{\beta_{sound}} \tag{11}$$

$$\frac{R_0}{R_{0,sound}} = a_R N_{eq} + 1 \tag{12}$$

where the parameters a_d, a_β, a_R are model parameters that are assumed to depend on concrete characteristics (e.g. porosity), β_{sound} and $R_{0,sound}$ are respectively the values of parameters β and R_0 for sound concrete, while N_{eq} is equal to the actual number N of the FTC if the concrete is subjected to frost deterioration conditions according to "Procedure A" described in ASTM C 666 [10]; according to this procedure, the specimens are both frozen and thawed in water in order to provide a very severe freeze-thaw condition being the specimen saturated. Otherwise, if different frost deterioration conditions are applied (e.g. freezing and thawing velocity, moisture content, etc.), N_{eq} represents the equivalent number of FTC according to ASTM C 666 "Procedure A" which leads to the same strength reduction. In this stage of the research the following relation is proposed for the evaluation of N_{eq}:

$$N_{eq} = \chi N^{\gamma} \tag{13}$$

where N is the actual number of FTC, while χ and γ are parameters that are assumed to depend on the experimental conditions according to which the FTC are performed.

The effect of different values of the parameters in equations (10)-(12) is depicted in Figure 2, while the effect of different values of the parameters of equation (13) is shown in Figure 3. The parameters a_d , a_β and a_R, that are assumed to depend on concrete characteristics, reflect the experimental evidence of increasing of frost-resistance together with quality of concrete. In particular, according to experimental evidences (e.g. [3]), stronger concrete exhibits lower a_d , higher a_β, is more resistant to frost action and shows an increasing strain peak shift. The parameters χ and γ account for different experimental conditions according to which the FTCs are performed and for possible non-linear relation between the degradation and the actual number of FTC, N [5].

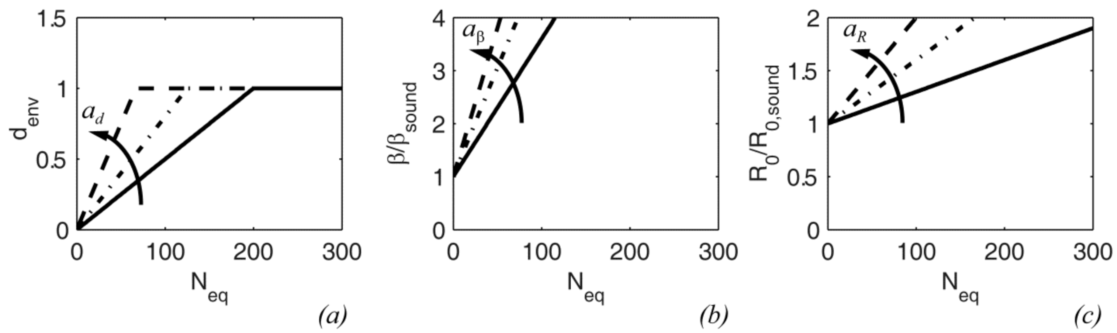

Figure 2: Effect of different concrete characteristics on frost damage model

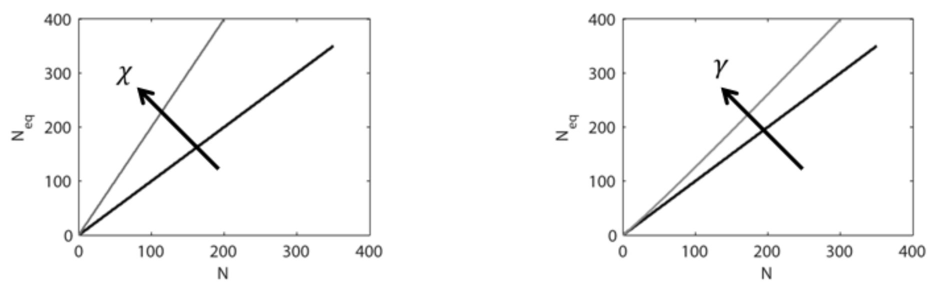

Figure 3: Effect of different values of parameters χ and γ on equivalent number of cycles N_{eq}

4 CALIBRATION OF FROST DAMAGE MODEL

In a previous work, [6], the authors focused on the compressive behavior of frost damaged concrete and calibrated the parameters of the model considering a limited number of experimental tests on concrete specimens under FTC. In the present work, more experimental results are considered.

4.1 Shang and Song experimental tests

The first experimental results considered were obtained by Shang and Song [1]. They tested plain concrete cubes under uniaxial and biaxial compression. Compressive strength of sound concrete at 28 days was 34.2 MPa, while the tensile strength, evaluated by means of direct tension test, was 3.14 MPa. The specimens were submerged in water before the exposition to FTC which were performed according to GBJ82-85 Standard [11] which is similar to ASTM C 666 “Procedure A”. Thus it can be assumed $\chi = 1$ and $\gamma = 1$ in (13) and $N_{eq} = N$.

Considering some of the experimental results, with an optimization procedure that minimized a cost function that represented the error between the numerical and the experimental stress-strain curves, the following relations were proposed [6]:

$$d_{env} = 0.005N_{eq} \leq 1 \tag{14}$$

$$\frac{\beta}{\beta_{sound}} = 0.026N_{eq} + 1 \leq \frac{1}{\beta_{sound}} \tag{15}$$

$$\frac{R_0}{R_{0,sound}} = 0.003N_{eq} + 1 \tag{16}$$

The other experimental results were used in order to validate the proposed equations. In particular, of the twenty experimental tests for different stress rations ($\alpha = \sigma_3/\sigma_2$) and different level of frost degradation, i.e. different number of FTC, six were used to calibrated the parameters, while the other fourteen points are profitably predicted by the proposed coupled model as it is evident from Table 1 where it can be seen that the mean error on strength is about -3.5% and the maximum error is -18.8%.

Table 1: Biaxial and uniaxial compressive tests of frost damage concrete: error between numerical and experimental results

	α=0	α=0.25	α=0.5	α=0.75	α=1
N=0	-2.1%	-8.0%	-3.8%	2.8%	-2.1%
N=25	-0.7%	-10.0%	-0.9%	4.3%	-0.6%
N=50	4.2%	-3.6%	-1.9%	5.8%	3.7%
N=75	-7.3%	-18.8%	-14.2%	-8.8%	-7.3%

The results obtained are reported also in Figure 4 in terms of failure points in stress-α plane and principal stress plane. As it can be seen the model is able to capture the overall behavior: in particular the ratio between biaxial strength and uniaxial strength increased with increasing number of FTC. On the other hand the model in general underestimates the strength for different values of α. The shape of the experimental failure surface is quite dissimilar for different number of FTC, while the difference in failure surface shape is less evident in the numerical model.

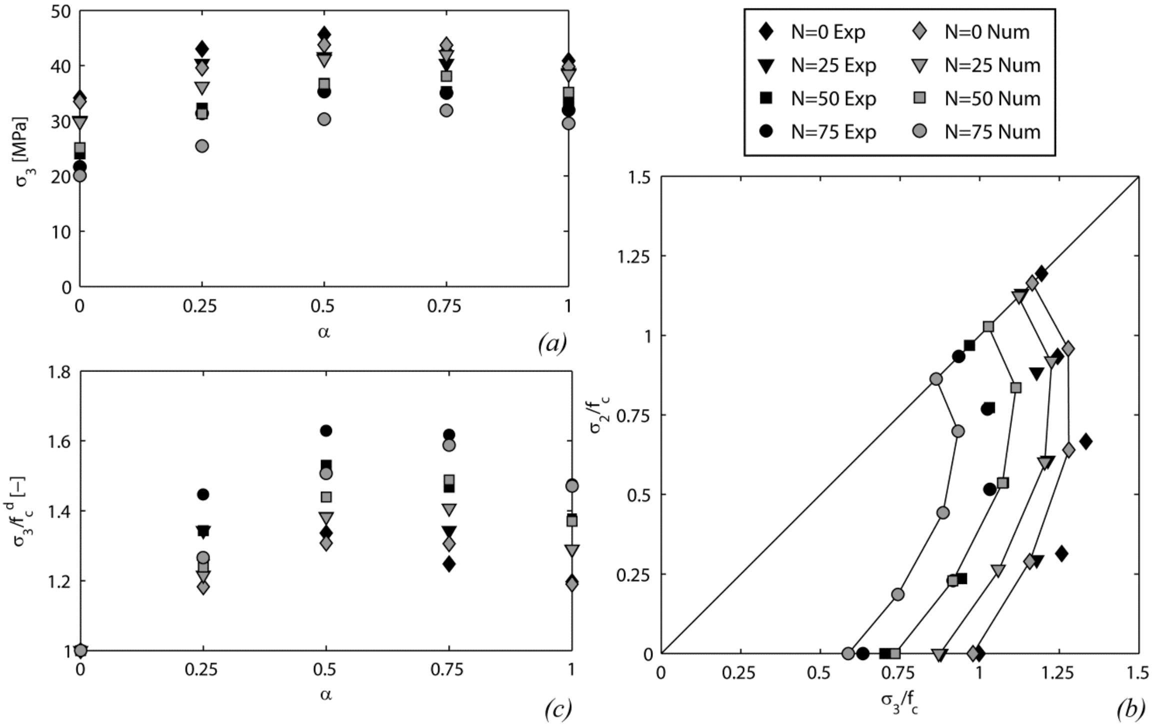

Figure 4: Experimental and numerical results compared in: (*a*) stress - α plane; (*b*) principal stress plane; (*c*) σ_3/f_c^d - α plane

4.2 Duan et al. experimental tests

Duan et al. [3] tested plain concrete specimens under uniaxial compression. In their study, they considered three series with different values of w/c ration. Series PAF was denoted by a w/c ratio of 0.60 and a compressive strength of 33.1 MPa. Series PBF corresponds to a w/c ratio of 0.54 and a compressive strength of 37.5 MPa. Finally series PCF was characterized by a w/c ratio of 0.48 and a compressive strength of 46.8 MPa. The freezing-and-thawing procedure was performed also in this case according to GBJ82-85 [11], allowing to consider $\chi = 1$ and $\gamma = 1$ in (13) leading to $\mathrm{N_{eq}} = N$.

Concrete of series PAF is similar to the one used by Shang and Song [1], thus the same values of parameters a_d , a_β and a_R are assumed. With such an assumption the results of series PAF are used as further validation of the previously proposed equations. The compressive strength reduction due to frost action, considering equations (8) and (14), may be written as:

$$\frac{f_{c,d}}{f_{c,sound}} = 1 - d_{env} = 1 - 0.005 N_{eq} \tag{17}$$

Figure 5 shows that the model predicts quite well the strength degradation for this series. Considering the other two series, the model parameter a_d is calibrated with a similar procedure to the previous case. It is possible to see that the model is able to represent the effect of frost action even on different concrete.

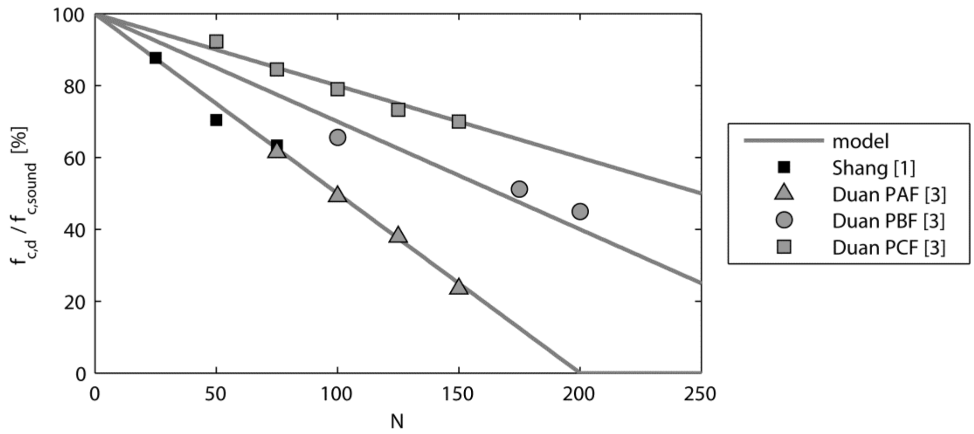

Figure 5: Compressive strength degradation: comparison between experimental and numerical results

5 FROST DAMAGED BEAMS

The proposed coupled environmental-mechanical damage model was applied to evaluate the load carrying capacity of RC beams tested by Hassanzadeh and Fagerlund [12]. They tested twelve beams characterized by two different geometries (small and large series), and different reinforcement ratios and stirrups. Concrete was similar to the experiments of Shang and Song [1], thus the same values of parameters a_d , a_β and a_R are assumed.

It is worth noting that in the experimental program, the damage beams were vacuum treated, submerged in water and then subjected to two freeze-thaw cycles [12]. In fact it was observed that if the critical saturation degree is reached, concrete undergoes heavily damaging even with one FTC (e.g. [2]). During usual open tests (like ASTM C 666 “Procedure A”), the specimen increases its saturation degree during the cycles. Thus the freezing-and-thawing procedure is very different and the equivalent number of cycles N_{eq} needs to be evaluated. The parameters χ and γ were estimated considering the degradation of strength experimentally observed on specimens drilled out from a block subjected to the same procedure. The values proposed in this work are χ=50 and γ=1 leading to $N_{\mathrm{eq}} = 50N = 100$. In this stage of the research limited information were available for tensile strength reduction due to FTC.

In the present work four beams, two reference and two damaged, were analysed. In particular specimens R1, R3, D1 and D3 were selected. They are simply supported beams with 4.4 m span and two concentrated loads with a shear span of 1.7 m. The cross section is (0.2 x 0.5) m^2 for both series. Beams 1 reinforcement consists in 4Φ20 longitudinal bars and 28 Φ8 stirrups. Beams 3 reinforcement consists in 6 Φ20 longitudinal bars and 32 Φ8 stirrups. In Figure 6 the geometry of the large beams (R1 and R3) is depicted.

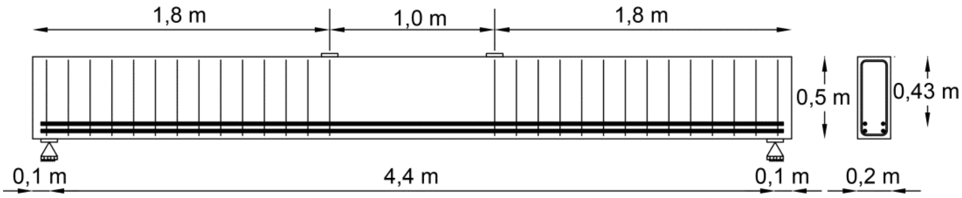

Figure 6: Geometry of large RC beams [12]

The beams are modeled with four point plane stress elements for concrete. The longitudinal reinforcement and stirrups are embedded in concrete elements assuming perfect bond between the two materials. Due to geometrical symmetry of beam, half beam is simulated. The input parameters of the coupled damage model for the beams are summarized in Table 2, while for the steel an elastic-plastic law with kinematic hardening is assumed, with Young Modulus E= 200.000 MPa, Hardening Modulus H = 2.000 MPa, yield stress fy= 670 MPa.

Table 2: Material properties adopted

E	33000	MPa
ν	0.18	
f_{c1D}	-37.6	MPa
f_{01D}/f_{c1D}	0.65	
$R_{0,sound}$	1.2	
f_0^+	3.6	MPa
β	0.3	
G_f	139	N/m

The results for beams R1 and D1 in terms of load-displacement curves are depicted in Figure 7 where they are compared with the experimental ones. It is possible to see that the model is able to capture well the global behavior predicting correctly failure load and displacement. The initial stiffness seems to be overestimated but it is worth noting that its value correspond to the gross uncracked section stiffness that has been evaluated analytically. Moreover the experimental stiffness is well approximated by the cracked section stiffness, suggesting a possible initial pre-cracking state of the beam, as frequently occurs in experimental tests. The global behavior of beam D1 is acceptably captured; in particular failure load and failure displacement are profitably predicted, while initial stiffness is overestimated. Comparing the curves for reference and damaged beam, together with the damage contour maps depicted in Figure 8(a) and (b) for beams R1 and D1 respectively, it can be noted that the proposed model is remarkably able to capture also the change in failure mode (from a ductile one to a brittle one) due to frost degradation: the damage distributions on beam R1 is typical of a ductile flexural failure, while the damage distributions on beam D1 suggest the failure of the specimen due to crushing of concrete in compression, according with experimental observation.

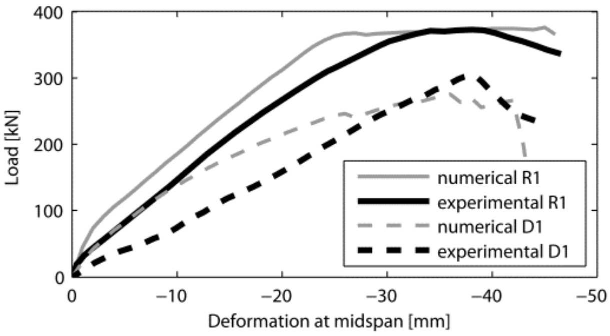

Figure 7: Load-displacement curves for beams R1 and D1

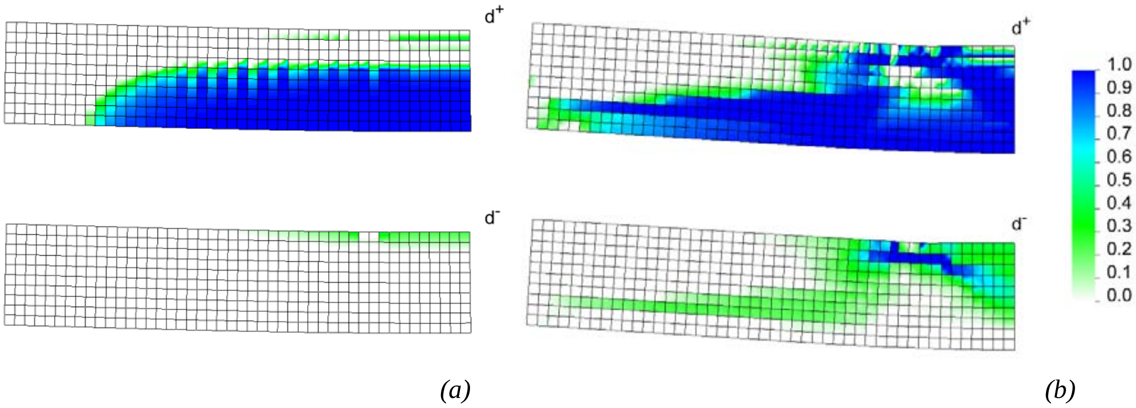

Figure 8: Damage contour maps for: (*a*) beam R1; (*b*) beam D1

The results obtained for beams R3 and D3 are pictured in Figure 9 where they are compared with the experimental load-displacement curves. The model is able to describe the behaviour of the reference beam (R3) quite well. In particular the failure load and displacement are well captured by the numerical model. Since beam R3 was highly reinforced, it failed due to crushing of concrete (brittle failure). The model is able to describe the failure mode (Figure 10a).

Concerning damaged beam D3, the model captures acceptably well the failure load and the failure mode which is due to crushing of concrete in compressive zone. In fact the failure load is slightly overestimated (+10%), while the failure displacement is sensibly overestimated with an error of about +85%. Similarly to the case of beam D1 the model overestimates the stiffness of the degraded beam in the first part. It should be noted that the degradation of bond due to frost action is not accounted in the model. Hanjari et al. [4] noticed a failure of anchorage at support for beam which may explain the overestimation obtained with numerical analysis. Furthermore in this stage of the research the reduction of tensile strength is captured only in an approximate way since it is assumed equal to the reduction of compressive strength. An enhancement of the model will be the introduction of an appropriate variable to take into account in a more refined way the reduction of tensile strength. A first attempt has been done considering the experimentally observed reduction of splitting tensile strength obtaining the preliminary result depicted in Figure11.

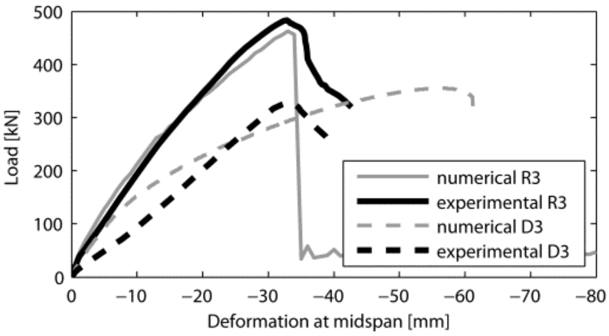

Figure 9: Load-displacement curves for beams R3 and D3

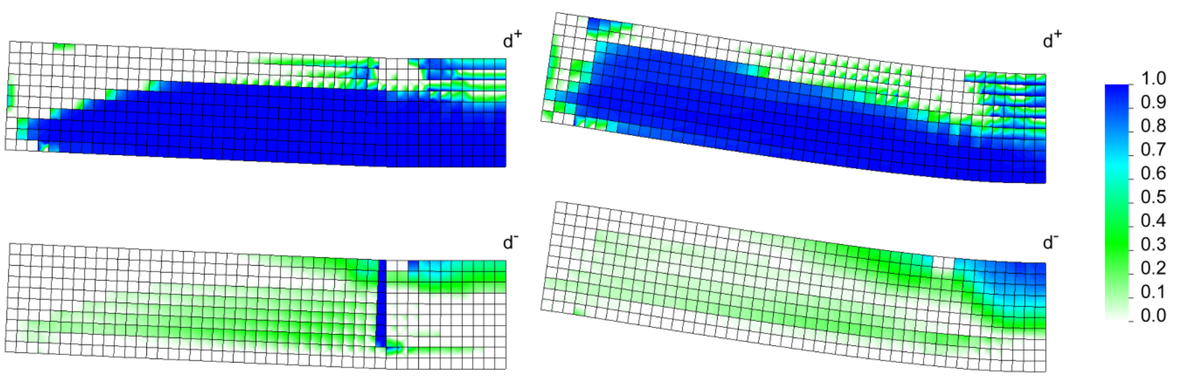

(a) *(b)*

Figure 10: Damage contour maps at failure for: (*a*) beam R3; (*b*) beam D3

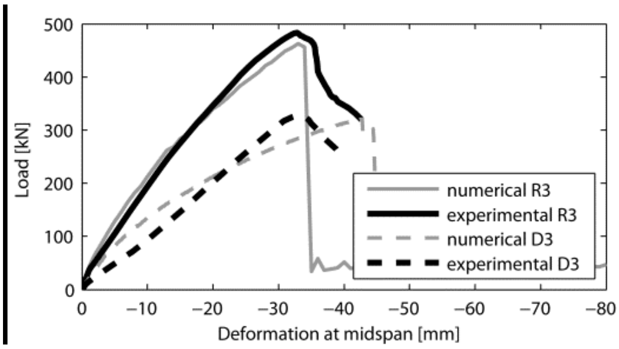

Figure 11: Load-displacement curves for beams R3 and D3

12 CONCLUSIONS

In the present work a coupled environmental-mechanical damage model, enhanced to take into account frost degradation process is presented.

The model is able to take into account some of the experimentally evidenced effects of FTC on concrete; in particular the model considers the reduction of tensile and compressive strength, the reduction of elastic modulus, the increasing of peak strain and the increasing of biaxial over uniaxial strength ratios with the increasing level of frost degradation.

The model was calibrated using experimental data from different research groups. It is worth noting that the number of tests considered is still limited and more experiments should be considered as soon as they are available.

Finally the proposed model was used as a predictive tool to simulate different experimental tests. The comparison between experimental and numerical results shows that the model can be considered an effective tool for assessing of structural behaviour of frost damaged RC elements.

At the present state the model does not account for the reduction of bond strength with increasing level of frost deterioration. Moreover it does not take into account the degradation of tensile strength in an appropriate way. Thus the model needs to be enhanced in order to better represent the effects of FTC on tensile behaviour and on bond-slip between concrete and steel as experimentally evidenced.

REFERENCES

[1] Shang, H.S., Song, Y.P. Experimental study of strength and deformation of plain concrete under biaxial compression after freezing and thawing cycles. *Cem. Concr. Res.* (2006) **36**: 1857-1864

[2] Fagerlund, G. Freeze-thaw resistance of concrete destruction mechanisms. *Report TVBM-3060* (1995) Div. Building Materials, Lund Institute of technology.

[3] Duan, A., Jin, W., Qian, J. Effect of freeze-thaw cycles on the stress-strain curves of unconfined and confined concrete. *Mat. Struct.* (2011) **44**: 1309-1324

[4] Hanjari, K.Z., Kettil, P., Lundgren, K. Modeling the structural behavior of frost-damaged reinforced concrete structures. *Struct. Infrastruct. Engng* (2013) **9**: 416-431

[5] Hanjari, K.Z., Utgenannt, P., Lundgren, K. Experimental study of the material and bond properties of frost-damaged concrete. *Cem. Concr. Res.* (2011) **41**: 244-254

[6] Berto, L., Saetta, A., Scotta, R. and Talledo, D.A. A coupled damage model for R.C. structures: proposal for a frost deterioration model and enhancement of mixed tension domain. *Submitted* (2013).

[7] Saetta, A., Scotta, R., Vitaliani, R. Coupled environmental-mechanical damage model of RC structures. *J. Engng. Mech.* (1999) **125**: 930-940.

[8] Talledo, D.A. A coupled environmental-mechanical damage model for structural analysis of RC constructions, *PhD Thesis*, Universities of Florence and of Braunschweig (2013).

[9] Faria, R., Oliver, J. A rate dependent plastic-damage constitutive model for large scale computations in concrete structures. *Monografia CIMNE*, 17, Barcelona (1993).

[10] American Standard ASTM C 666. Standard Test Method for Resistance of Concrete to Rapid Freezing and Thawing (1997).

[11] GBJ82-85. National Standard of the People’s Republic of China, The Test Method of Long-Term and Durability on Ordinary Concrete (1997).

[12] Hassanzadeh, M., Fagerlund, G. Residual Strength of the Frost-Damaged Reinforced Concrete Beams. *III European Conference on Computational Mechanics* (2006)